applied sciences

MDPI

Review

A State-of-the-Art Review on Robots and Medical Devices Using Smart Fluids and Shape Memory Alloys

Jung Woo Sohn [1], Gi-Woo Kim [2] and Seung-Bok Choi [2,*]

[1] Department of Mechanical Design Engineering, Kumoh National Institute of Technology, Gumi 39177, Korea; jwsohn@kumoh.ac.kr

[2] Department of Mechanical Engineering, Inha University, Incheon 22212, Korea; gwkim@inha.ac.kr

* Correspondence: seungbok@inha.ac.kr

Received: 21 September 2018; Accepted: 14 October 2018; Published: 15 October 2018

Abstract: Over the last two decades, smart materials have received significant attention over a broad range of engineering applications because of their unique and inherent characteristics for actuating and sensing aspects. In this review article, recent research works on various robots, medical devices and rehabilitation mechanisms whose main functions are activated by smart materials are introduced and discussed. Among many smart materials, electro-rheological fluids, magneto-rheological fluids, and shape memory alloys are considered since there are mostly appropriate application candidates for the robot and medical devices. Many different types of robots proposed to date, such as parallel planar robots, are investigated focusing on design configuration and operating principles. In addition, specific mechanism and operating principles of medical devices and rehabilitation systems are introduced and commented in terms of practical realization.

Keywords: smart materials; actuators; robots; electro-rheological fluids; magneto-rheological fluids; shape memory alloys; medical devices; rehabilitation system

1. Introduction

Historically, material technologies have had a profound influence on human civilization, and hence historians have defined distinct time periods by the dominant materials used during those eras. The term 'smart materials' first appeared in the late 1980s, and since then, a multitude of research activities on smart materials has been, or is being, conducted in diverse industry areas. Among the many inherent characteristics of smart materials, the crucial common denominators to achieve high performances in application systems are their capabilities of sensing, actuating, and controlling under external stimuli that govern the responses of the systems. To date, more than 100 types of smart materials with these capabilities have been proposed, and their adaptability as 'smart' has been validated. These include the identification of material characteristics showing sensitivity as sensors, generating forces as actuators, and performing control responses as a controller. In the last two decades, several classes of smart materials have received significant attention, over a broad range of engineering applications, because of their unique and useful actuator properties. Potential smart materials for robotic and medical applications include electro-rheological (ER) fluids (ERFs), magneto-rheological (MR) fluids (MRFs), and shape memory alloys (SMAs). It is noted here that ERFs also include homogeneous types such as liquid crystal in the sense of the electric field response smart material. However, in this review article, ERFs which can be expressed by Bingham model, in which the field-dependent yield stress is the dominant behavior, are considered only.

In the robotic research society, many researchers have developed various types of robots using traditional actuators (e.g., electric motors, hydraulic fluidic actuators) to achieve some specific

requirements for desired movements. Although some robots with conventional actuators have demonstrated excellent performance, alternative actuators need to be explored when the capability to perform flexible and complex movements is required. Smart material-based actuators are one of these alternative solutions, because of their relatively small weight and volume, compared to those fabricated using conventional actuating methods. For example, SMAs have been widely used in a diverse range of humanoid-robotic applications since the 1980s, especially as artificial muscles, because SMA wire actuators can mimic the human muscle. The use of smart materials as actuators can be categorized in terms of their application areas: automotive, aerospace, robotics, and medical, amongst others. Despite numerous research works on smart materials applications, a comprehensive overview on the specific application areas of diverse robots, medical devices and rehabilitation systems is not readily available. Therefore, it is worthwhile to timely review one of attractive applications of smart materials, namely robot and medical applications.

Consequently, the main objective of this review article is to present a broad perspective of the research efforts during the last two decades in relation to robot and medical devices, and their prototypes, based on ERFs, MRFs, and SMAs. This review describes the attributes of specific smart materials that make them ideal for actuating robotic and medical applications, and discusses their associated technical capabilities and limitations in order to emphasize the design challenges. Therefore, this article provides an updated review of recent smart material research of robot and medical applications, with 100 state-of-the-art references categorized into three types of smart materials. It is remarked here that this review article is focused on the operating principle and design concept of each application for easy understanding of the potential readers of this attractive research field, instead of the specific dynamics and control strategies of the adopted devices and systems.

2. Robots Using ERF and MRF

2.1. Material Characteristics

ERFs are a class of colloidal dispersions that exhibit a large reversible change in their rheological behavior when subjected to external electric fields. These changes in rheological behavior are manifested by a dramatic increase in flow resistance, which depends upon the flow regime and the composition of the ERF. The flow resistance can be considered an actuating force controlling dynamic motions, such as vibration and position. In order to achieve flow resistance, ERFs are frequently modeled by a simple Bingham plastic model, in which the field-dependent yield stress is expressed as a controllable resistance. Among the many inherent characteristics of ERFs, the most salient property is the fast response of the actuating force (or torque) caused by application of an external electric field. This important property has triggered numerous application research works on ERF, including automotive shock absorbers, brakes, clutches, and smart structures. In addition, owing to their fast and easy controllability, ERFs are applied to robot systems, where they are embedded into the flexible arms of manipulators. Some other applications of ERF in robotic areas include tactile sensors, and human-friendly soft hands. It is also known that, when subjected to an external magnetic field, MRFs have exactly the same characteristics as ERFs. The rheological properties of MRFs, such as complex moduli, can be tuned or controlled by changing the intensity of the magnetic field associated with appropriate control schemes. Thanks to the robustness and higher material performance of MRFs compared to ERFs in a practical environment, numerous studies on the applications of MRFs are being actively undertaken in many industrial fields such as automotive, aerospace, and civil engineering. MRFs have a much higher field-dependent yield stress than ERFs, and hence, they satisfy the force or torque requirements of many practical systems or devices over a wide temperature range. However, MRF has slower response time compared to ERF. Moreover, the weight of MRF-based devices is much heavier than ERF-based devices because of high density of ferromagnetic metals.

2.2. ERF-Based Robots

As far as is known, the first application of ERFs to robotic systems was reported by Gandhi et al. [1]. In this work, the forearm of a commercial parallel robot was retrofitted by inserting ERF. The deflection of the forearm was successfully reduced during dynamic maneuvering and transient motions, owing to the increment of the field-dependent damping property of the ERF domain. Choi et al. [2,3] performed a study similar to Gandhi et al. [1], with primary focusing on the vibration control of a flexible robot arm incorporating ERF. In this work, a single-link flexible robot arm system was made by inserting ERF into the box-type aluminum arm. The simulation and experiment were both conducted to evaluate effective control of the transient vibration during a rotational maneuver. A number of other studies were conducted using the same concept for vibration control of a flexible gantry robot [4,5]. In the gantry robot system, the translational motion was controlled by a bi-directional ER clutch, and the vibration due to the flexibility of the link was controlled by a piezoelectric actuator bonded on the surface of the link. As for the controller, a robust, H-infinity controller was designed and built, using a microprocessor. Excellent positional and vibrational control responses were achieved in the presence of uncertain system parameters, such as the variation of natural frequencies. Monkman [6] proposed a high-resolution tactile display using ERF, applicable to the virtual reality (VR) environments encountered underwater or in space exploration. Figure 1 shows a compressive-type tactile display whose hardness can be tuned by the electric field and the changed hardness can be felt by fingers exploring the surface. The movement of the fingers over the surface allows the shape of an object to be detected by touch, with the regions that correspond to the position of the object being harder than those outside the image. In Figure 1, the white circles represent the dielectric separating mesh. The dielectric separating mesh is essential to prevent the earthed compliant surface from coming into direct contact with the uncharged tactor elements resulting in a short circuit when they become activated. More recently, a study on the feasibility and suitability of an ERF-based actuator in human-friendly manipulators was reported in [7]. In this work, the actuator criteria were checked, based on ERF properties and the application of an ER clutch. It has been shown that ERFs exhibit promising characteristics for use as robotic actuators. Specifically, they are well suited for actuation systems that interact physically with humans, because of their inherent characteristics such as intrinsic back-drivability, low-output inertia, superior performance and bandwidth, and precision controllability of output torque. The state-of-the-art robotic applications using ERF actuators are summarized in Table 1.

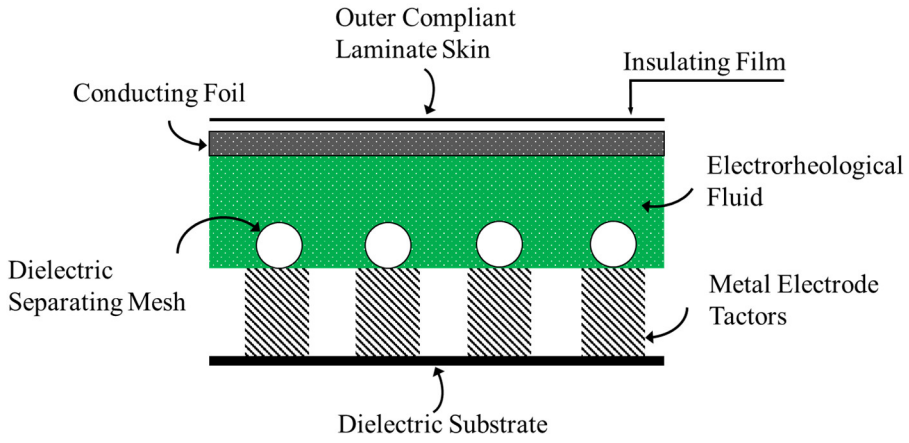

Figure 1. Tactile display featuring ERF [6].

Table 1. Summary of state-of-the-art robotic applications using ERF.

Robot	References
Flexible robot arm	[1–3]
Flexible gantry robot	[4,5]
Tactile display	[6]
Manipulator	[7]

2.3. MRF-Based Robots

MRFs have been for the first time applied to vehicle shock absorbers, and some of the passenger vehicles integrated with MR dampers are currently available on the market [8,9]. The application of MRFs to robotics has been actively researched since 2000. Initially, the feasibility of MRFs as robotic actuators was both conceptually and experimentally studied [10]. There are two possible approaches when investigating the actuating characteristics of MRFs. One is to make valve systems and produce an active control force in closed-loop systems. The other is to directly use MRFs as actuators, by generating a flow motion in three different flow modes (flow, shear, and squeeze), in which a semi-active damping force is normally produced in open- or closed-loop control systems. Recently, Yadmellant and Kermani [11] proposed a new adaptive control method to compensate for the inherent hysteretic phenomenon of MRFs, and to develop high-performance robot actuators. In order to validate the proposed control scheme, a small-sized two degrees-of-freedom (2-DOF) MR-actuator robot manipulator was manufactured, and the higher accuracy of its torque-control results, compared to the case without the hysteretic compensator, was presented with various frequency torque trajectories.

The state-of-the-art robotic applications using MRF actuators are summarized in Table 2. A robot application device with MRFs, a deformable gripper that handled implements such as a writing pen, was invented in [12]. This gripper could be deformed in conformance with the user's hands and fingers, with the gripper comprising a tubular sleeve in which the MRF flowed radially. The deformability of the gripper was controlled by a sliding mechanism activated by an electromagnet. A robot gripper for handling delicate food products using MRFs was also developed in [13]. In this work, a two-finger gripper was manufactured. When the MRF, in pouches, reached the sides of the object, the pouches started to deform without stretching the pouch material. One of the gripper arms was fitted with a strain-gauge force sensor, which allowed for multiple gripping modes. The gripping force when handling various fruits and vegetables, such as carrots and strawberries, was measured through both open-loop setting speeds and closed-loop control methods, associated with a proportional–integral–derivative (PID) controller. It was concluded that the gripping force was evenly spread over a large surface, reducing the risk of bruising, and that the geometric dimensions of the gripper were crucial in achieving a universal gripper, able to handle any size or shape of food products. More recently, Nguyen et al. [14] proposed a new type of 3D-haptic gripper for tele-manipulation, using an MR brake system. This haptic gripper transfers the rolling torque, grasping force, and approach force from the slave manipulator to the master operator. Figure 2 shows a schematic configuration of the 3D-haptic gripper which can be applied in surgical robots, where the gripper is attached to a stationary base, and the master manipulator and the haptic gripper are separated. The haptic gripper consists of two rotary MR brakes. These are the grasping and rolling MRBs, and two identical linear MRBs to reflect the approach force. The shaft of the rolling MRB is fixed to the body of the haptic griper while its housing is attached to the stationary base. The shaft of the grasping MRB is connected to gear 2 while its housing is fixed to the gripper body. The gear 2 externally mates with gear 1. On gears 1 and 2, the two shafts of the linear MRBs are attached. The housings of the linear MRBs, on which the handles of the gripper are attached, can move relative to their shafts. By controlling the applied currents of the MRBs according to signals received from the slave sensors, the grasping force, rolling torque and approach force from the slave can be reflected to the human operator [14]. In this work, the principal design parameters, such as the magnetic pole, are determined

by an objective function considering both the off-state braking torque/force, and the mass of the brake itself.

Table 2. Summary of state-of-the-art robotic applications using MRF.

Robot	References
Manipulator	[11]
Deformable gripper	[12,13]
Haptic robot	[14–18]
Rehabilitation	[19–22]
Collaborative robot	[23–28]
Planar robot	[29]
Climbing robot	[30]
Spherical robot	[31]

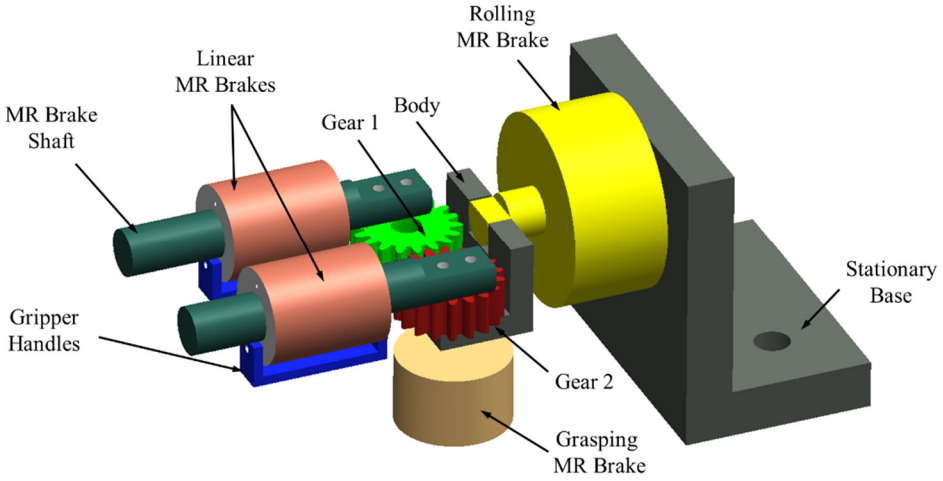

Figure 2. 3-D haptic MRF gripper for surgical robot applications [14].

An innovative haptic display for whole-hand immersive exploration was proposed, and its practical feasibility was demonstrated via a conceptual experiment proposed by Scilingo et al. [15]. In this work, a haptic black box, which can be imagined as a box into which the operator can poke his or her bare hand, was devised using MRFs and its effectiveness was tested through psychophysical experiments to assess performances of softness and shape. A compact haptic glove using MR brakes was developed and its time required to grasp a virtual object was investigated with a force feedback controller by Blake and Gurocak [16]. The proposed glove was made using six MR brakes to generate the movement three fingers, and four-bar mechanisms, to connect the brakes to the digits of the fingers. In the design process of the glove, easy controllability of the fingers, minimization of user fatigue, user's safety, and freedom of motion were considered for satisfying the general requirements of the force feedback gloves. The thumb, index finger, and middle finger are attached to two MR brakes in which the motion of the thumb is constrained to 2-DOF. The braking torque is then transmitted to each finger joint by using the four-bar linkage, which allows the MR glove to be adjusted to different hand sizes. The effectiveness of the MR glove, which weighs 640 g, was evaluated by two different methods: virtual object manipulation, and by reflecting the stiffness of a virtual object held between two fingers. It was shown that the task completion times were reduced by 79% by activating the MR glove, and the difference in stiffness of the springs was identified with a higher percentage of success. Several works on robotic systems closely related to medical surgical applications have been performed utilizing MRF technology. For applications in robotic surgery, a new type of 5-DOF MRF-based tele-robotic haptic was proposed and applied to remotely control a slave robot by Ahmadkhanlou et al. [17]. In this work, after analyzing the MR structure, a force feedback control was employed to replicate in the master, those forces encountered in the slave. Recently, using the salient property of the variable impedance

of MRFs as a function of a magnetic field, a series-clutch element was devised for autonomous and tele-robotic operation by Walker et al. [18]. In this work, a series-clutch actuator, which transfers torque up to some saturation level, was made by utilizing a clutch between the DC motor and output link. After experimentally identifying its step response and hysteretic behavior, the clutch was modeled as a first-order system, and a combined tele-robotic control architecture, to reduce the impact force, was formulated and implemented. It was shown that unwanted impact, or collision forces, at the output, are significantly reduced by activating the proposed system, which in turn indicated a great improvement of safety in uncertain environments, or with human contact.

One potential application of MRF technology in the robotic area is in rehabilitation elements or components. Over the last decade, many studies on lower-limb rehabilitation, utilizing MR mechanisms such as clutches or brakes, were undertaken. Specifically, research work on lower-limb robotic rehabilitation related to various gait motions was performed by Diaz et al. [19]. It is known that many patients with cerebral lesions have a spastic movement disorder, which slows voluntary limb movement. This has led to much research on lower-limb rehabilitation using servo-motors. However, it is challenging to guarantee both stability, and powerful motion, by employing a servo-motor-based leg system. Kikuchi et al. [20,21] proposed a haptic controllable leg-shaped robot (Leg-Robot) to be used by patients with spastic ankle joints. The Leg-Robot was made with an MR clutch, which provided a safety mechanism, and a haptic generator of the system. In the design process of the Leg-Robot, they considered mass characteristics at a level approximating that of elderly people (over 75-year-old males). Figure 3a shows the basic structure of the Leg-Robot, in which the MR clutch is built in the knee joint. It was demonstrated that the desired torque levels, corresponding to the spasticity mode and the ankle-clone mode, could be successfully achieved by controlling the MR brake. Jiang et al. [22] proposed a robot leg comprising a rotational MR damper, a torsional spring, a steel plate, and a curved part of the foot that makes contact with the ground, as shown in Figure 3b. As it walks, the foot rotates to form an angle between the core and outer cylinder of the MR damper, while the forces acting on the foot vary according to the synthesized effect of the driving torque of the motor on the axle, and to the dynamic force of the terrain acting on the foot. It was demonstrated that the vertical forces at different walking speeds can be controlled in real time to adapt to the surroundings by controlling the magnetic field applied to the MR damper. In this case, a higher angular speed than other tunable legs were achieved, due to the guaranteed stability associated with the semi-active control of the MR damper.

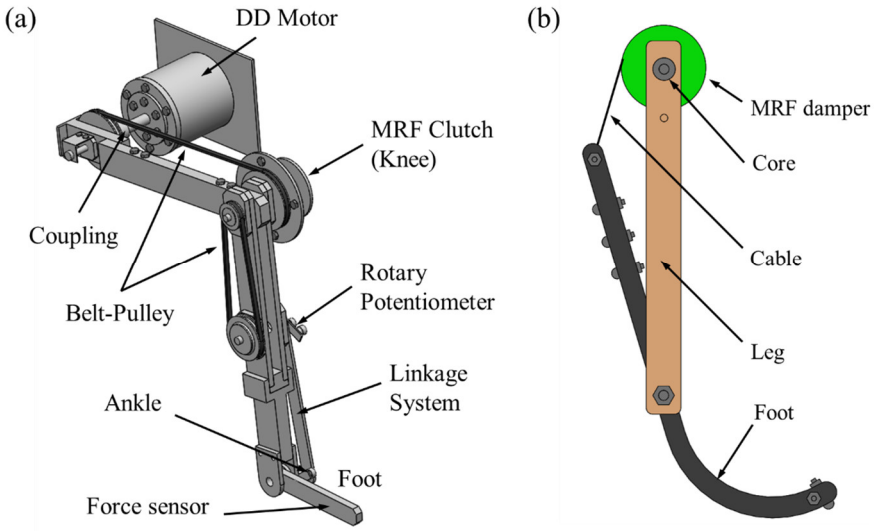

Figure 3. Leg-Robot using MR devices; (**a**) MR fluid clutch [20,21]; (**b**) MR fluid damper [22].

There are several types of collaborative robot systems for robot-to-robot or robot-to-human interactions. Specifically, a robot sharing its working space with humans has been actively researched for many purposes such as carrying heavy objects in factories. Saito and Ikeda [23] proposed a

MR-clutch type safety device for human-collaborative robots. In this work, an MR clutch comprising magnetic circuits associated with the permanent magnet and electromagnetic coil, yoke, rotor, and driving shaft was developed to achieve high levels of output torque. After verifying the safety function of the MR clutch, the transmitted torque of two different types, single- and triple-rotor, were evaluated as a function of the input current (magnetic field). They concluded that, in order to build a safety device capable of controlling the torque output of the robot joint axis and securing the holding torque in an emergency case, the proposed MR clutch was a promising candidate for practical implementation. Ahmed et al. [24,25] developed a robot-arm system featuring an MR clutch/brake to accomplish a safe human–robot interaction, which is a type of compliance control. Fauteux et al. [26] proposed a dual-differential rheological actuator (DDRA) to investigate the feasibility of high-performance robotic interactions, in which safety, robustness, and versatility are paramount. The DDRA was manufactured based on the synergistic use of two differentially coupled MR brakes, and an electromagnetic (EM) motor. After analyzing the DDRA in terms of output friction, torque level, backlash, and interaction force, a one-link manipulator was integrated with the DDRA, as shown in Figure 4, in order to control the joint torque, and hence the position of the manipulator. It has shown from the experiment that more accurate position control, higher torque bandwidth, and smaller inertia of the DDRA compared to conventional EM actuators can be achieved utilizing the DDRA. Shafer and Kermani [27,28] undertook a research similar to Fauteux et al. [26]. In these works, MR clutch actuators were proposed as promising candidates for human-friendly manipulators because of the clear benefits of MRFs. After surveying the actuator requirements for human-friendly manipulators, such as torque levels and control bandwidth, a distributed active semi-active (DASA) actuation mechanism, comprising a driving motor and semi-active MR clutch, was designed and manufactured. In the design process, the actuator inertia, mass of MR clutch, and output impedance were crucially considered in order to achieve maximum efficiency as a robot actuator. It was demonstrated, via experimental work, that accurate torque control with high control bandwidth could be achieved, thus validating an excellent actuator for human-friendly manipulators, which require intrinsic back drivability, low output inertia, and accurate control performance with high bandwidth.

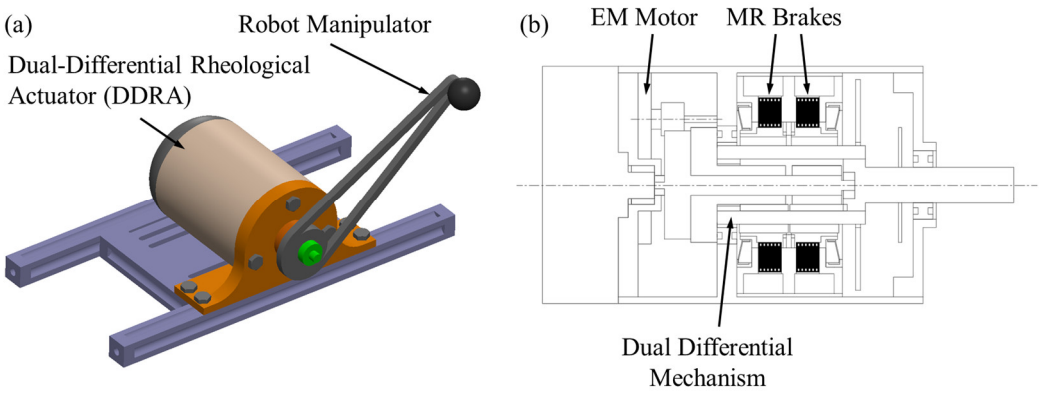

Figure 4. Robot arm featuring dual-differential MR actuator; (**a**) configuration (**b**) section view of DDRA [26].

A novel parallel-planar robot using an MR damper was developed, and its effectiveness was validated by demonstrating tracking control performance in the x–y plane by Hoyle et al. [29]. In this work, a linear motor and two MR dampers were used as actuators. The linear motor is responsible for moving the platform, while the MR dampers guide it through predefined paths by creating adjustable and controllable resistive forces. The platform then follows the path, based on the concept that moving objects intuitively tend to follow the direction that imposes minimum resistance against motion. Figure 5 shows the planar robot manufactured in this work. In order to demonstrate control accuracy of the robot, three different trajectories, straight, inclined, and sinusoidal, were adopted as those to be

followed by the robot, and excellent tracking control performance was achieved by implementing a PD controller. This work noted one salient property of the planar robot using an MR damper. If an excessive load is applied to the joints by an incorrect controller command, the joints and links will not be easily damaged because the MR dampers can easily absorb the majority of such loads. MR fluid technology has been extended to a controllable climbing robot, using the adhesive effects of MR fluids. Wiltsie et al. [30] developed a novel type of climbing robot using the field-dependent adhesive effect of an MR fluid. Before building the robot, they investigated the adhesion property of MR fluids with, and without, a magnetic field. From this test, the fluid thickness between two parallel plates was found to have little effect on the adhesive failure strength, and a positive effect on time to failure, while the target surface roughness and orientation were found to have a significant effect on pull-off adhesion, and a positive effect on shearing loads. In addition, in order to investigate the holding time of the MR fluid adhesive, a pseudo-creep test was undertaken, and the maximum allowed holding time until failure was identified as 5 min. They manufactured four feet using MRF, by considering the holding time, failure time, and surface conditions of climbing materials, and tested them on a vertical board covered with 150-grit sanding cloth. It was found in the test that the proposed robot could climb the vertical board with a shear of approximately 7.3 kPa, which was generated by activating the magnets. On the other hand, Yue and Liu [31] applied MRF technology to control unwanted oscillations of a spherical robot. In general, the inner suspension platform of a spherical robot undergoes a severe oscillation when the robot is rolling forwards, which could cause instability of the robot system. Thus, in order to reduce oscillations during the rolling motion, they used an MR damper integrated with a robust sliding-mode controller, which was robust against disturbances and parameter insensibility.

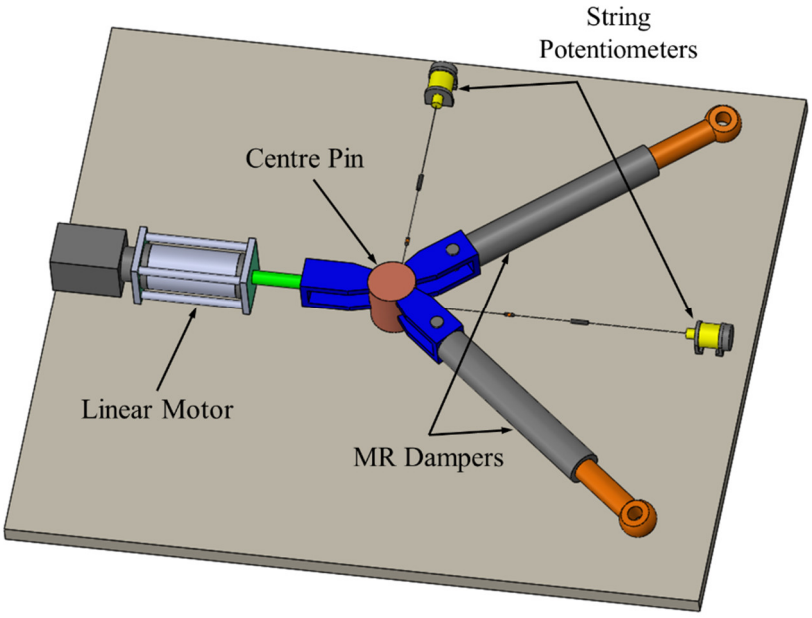

Figure 5. Schematic of parallel planar robot using MR damper [29].

One potential smart material, with material characteristics controllable by external magnetic fields, is the magneto-rheological elastomer (MRE). A controllable MRE, which belongs to the MR-material family, is a composite material with magnetic sensitive particles suspended, or arranged, within a non-magnetic elastomer matrix [32,33]. The operational modes of an MRE are quite different to those of MRFs in that the iron particles are locked within the polymeric matrix, and under external excitations. This restricts the particle movement around their original locations, and thus the direction of the chain structures no longer coincides with the magnetic field. The three operational modes of an MRE are classified as shear, squeeze/elongation, and field-active modes. Depending upon the dynamic motion of MRE applications, an appropriate operational mode needs to be selected to maximize actuating

performance. Recently, a new concept for locomotion of miniature robots, based on the periodic electromagnetic actuation of the MRE body structure, was introduced by Zimmermann et al. [34]. Figure 6 presents a basic configuration of two different micro-robots with MRE body structures. The left one incorporates an inelastic-polymeric frame with an integrated micro-coil, and the movement is bidirectional, controlled by the driven frequency. The right one consists of only a symmetric MRE body with six embedded micro-coils, and thus, is applicable to compliant planar-locomotion systems. In this work, prototypes of the two MRE activated micro-robots were manufactured, and their dynamic motions were investigated by observing the driven frequency-dependent movement for two cases, uniaxial- and the planar-locomotion systems. It was seen from the experiments that the maximum average speed of the uniaxial locomotion system was 4.1 mm/s at a driving frequency of 20 Hz, while that of the planar locomotion system was 5 mm/s, at the same driving frequency.

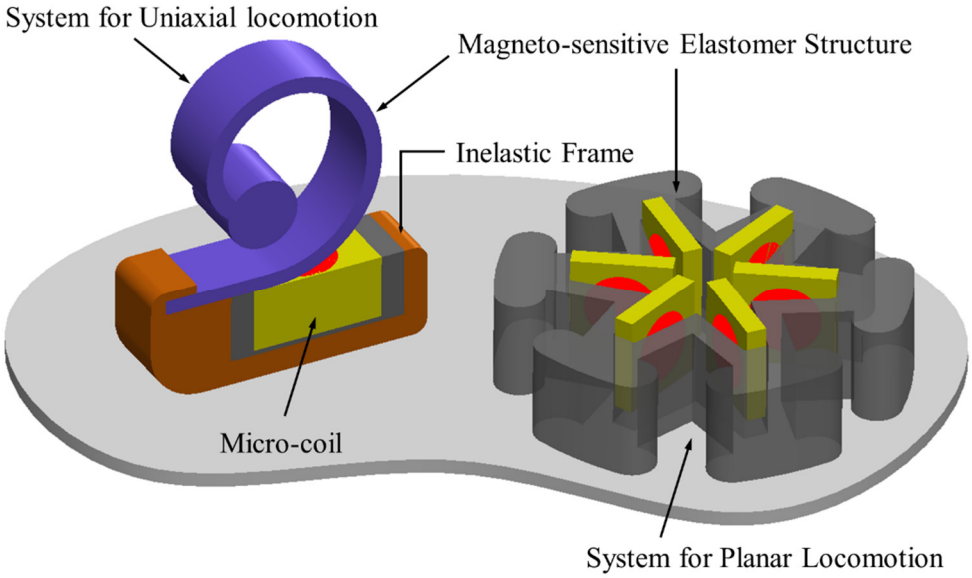

Figure 6. Two different micro-robots featuring MRE body structures [34].

3. Robots Using SMA

3.1. Material Characteristics

Shape memory alloys (SMA) are a class of metallic alloys that can return to their original shape because of the phase-transformation phenomenon, known as the shape memory effect (SME), when subjected to changes in temperature or magnetic field. The primary application of these materials is therefore in actuation systems, where the SMAs can be readily contracted or recovered to their original form. The actuating motions could be achieved by controlling temperature beyond a certain threshold temperature, by internal Joule heating. SMAs possess two different phases with three different crystal structures: twinned martensite, detwinned martensite, and austenite. Typically, the austenite phase is stable at high temperatures, and the martensite phase is stable at lower temperatures. Upon heating an SMA, the initial martensite phase begins to transform into the austenite phase, as shown in Figure 7. The onset temperature is A_s, where the austenite transformation starts, and A_f is the terminal temperature, where this transformation is complete. Once an SMA is heated beyond A_s, it begins to transform into the austenite structure, resulting in recovering (i.e., contracting) to its original shape. During cooling, the transformation starts to reverse to the martensite at M_s, and is completed when it reaches M_f. Above the highest temperature (i.e., A_f), SMA is permanently deformed, similar to ordinary metals and alloys. In addition, SMAs exhibit other shape-memory characteristics, such as pseudoelasticity or superelasticity. The SMAs can return to their original shapes after applying mechanical loading at temperatures between A_f and M_d, without any thermal

activation. This property is currently used for passive vibration-damping applications. Hysteresis is a measure of the difference in transition temperatures between heating and cooling, and is generally defined between the temperatures at which 50% of the material is transformed to austenite upon heating, and 50% is transformed to martensite upon cooling. This hysteresis has significant design considerations for SMA applications. For example, a small hysteresis is typically required for fast actuation applications, such as in robotics, while larger hysteresis may be required to retain the predefined shape, such as in deployable structures within a large temperature range. The hysteresis loop associated with different transition temperatures is known to be affected by the composition of the SMA material, and the thermomechanical processing. In addition, some of the SMA's properties also vary between these two phases, including the Young's modulus, electrical resistivity, thermal conductivity, and thermal expansion coefficient. Detailed information on the mechanical properties of SMAs is well summarized in relevant references [35–37].

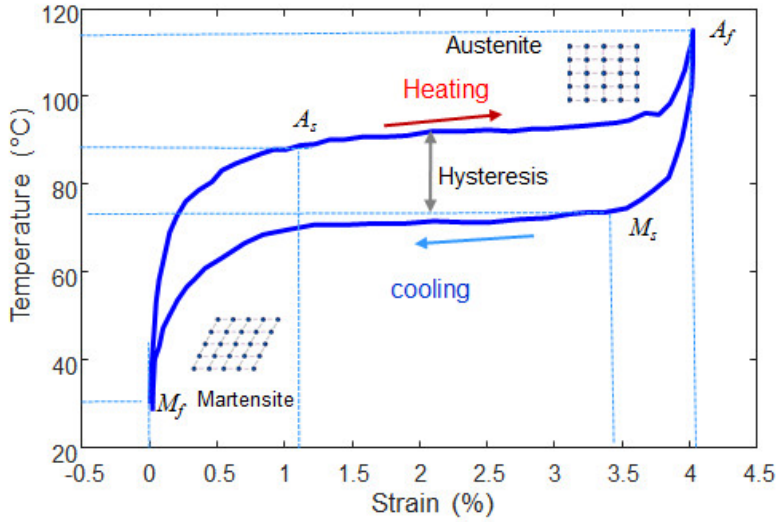

Figure 7. Typical phase transformation curve of SMA wire [35].

SMAs are particularly attractive for actuator applications because their strain (length change or stroke) during the contraction phase is relatively larger than other smart materials, such as piezoelectric transducers, and it is typically 4–5% of their initial length. If the contraction is constrained, large block forces can be generated, and stresses may reach the order of magnitude of 1000 MPa. However, for actuator applications with a large number of load cycles, up to 10^5, the stress level should be alleviated, up to 200 MPa, to prevent fatigue damage. Compared to other actuation systems, high work output along with lower weight (i.e., high power density) can be achieved with SMAs, which is important for robot applications. While the temperature during the contraction process is controlled electrically through Joule heating, cooling is simply controlled by convection in surrounding air, which results in a much slower recovery response. This asymmetric actuation property limits SMA actuators to nearly quasi-static applications, with an actuation frequency of approximately 1 Hz. A few feasible solutions have been suggested to resolve this narrow bandwidth issue, including the use of heat sinks, as in Peltier cooling elements, heat conductive compounds, oil, or water with glycol [35]. However, the cooling rates are not very promising, and special additional devices are required. In addition, SMAs have another technical challenge associated with their lower energy efficiency. Theoretically, the maximum energy efficiency of SMAs is in the range of 10–15%, depending on actuation modes (i.e., loading type). As a result, SMA wire-actuator applications are limited to special areas where energy efficiency is not a significant issue.

3.2. SMA-Based Robots

SMA actuators for robotic applications can be categorized according to various actuation configurations in terms of loading types. Most of the actuator designs are based on an SMA spring-wire type, as a large stroke change can be generated with a relatively small microscopic strain, and because of its simplicity of fabrication, by annealing an SMA wire wound on a rod [38]. Most key parameters—such as the wire diameter, rod diameter, pitch angle, and number of active coils—can be successfully designed, based on reliable SMA models [39]. However, the stress distribution over the cross-section of an SMA spring is no longer constant, and therefore it requires greater material volume to generate the same force, which will have an effect on the efficiency and the bandwidth of the actuator. Therefore, a straight, linear wire type for tension loading is more advantageous because of its significantly higher efficiency (i.e., more work generated from a minimal amount of SMA material). Various versions of linear SMA wire actuators can be found in recent literature. For example, Flemming et al. [40] suggested a wet SMA actuator embedded within a compliant fluid-filled tube to produce a linear contraction and extension of the SMA wire. Zhang et al. [41] proposed a hybrid linear actuator by using an SMA wire and DC motor to resolve the low driving frequency issue. A new flexible SMA actuator, composed mainly of an SMA wire and a multilayer tubular structure, was proposed to make the conventional linear SMA wire actuator flexible, with high axial stiffness [42]. As robots have become a focus of interest, they are now required to complete various diverse tasks in a variety of environments, using factors such as a torsional motion. In order to produce a torsional (or twist) deformation, a smart soft-composite torsional actuator using SMA wires has been proposed by Shim et al. [43]. The proposed twisting actuator is composed of a torsional-restrained SMA wire embedded in the center of a polydimethylsiloxane matrix. Sheng et al. [44] proposed a torsion actuator composed of a pair of antagonistic SMA torsion springs, capable of bi-directional actuation. Rodrigue at al. [45] manufactured a hollow-tube-shaped actuator, with multiple curved SMA wires that follow the curvature of the tube, and which is capable of pure-twisting deformations, while sustaining a cantilever load. This wrist actuator showed twisting deformation up to 25° while holding objects weighing 100 g, and could sustain loads above 2 N without buckling. Recently, different loading types of SMA wire actuation have been explored for robotic origami applications, which require multiple sequential folding of tiled sheets for recovering the original shape. Paik et al. [46,47] presented a preliminary research on a low-profile bidirectional folding actuator based on annealed thin NiTi sheets (thickness of 0.1 mm), for meso- and micro-scale robotic applications. A torsional actuator composed of an SMA wire, with a diameter of 0.25 mm in the array form, and two supporting elements, was developed to provide large rotational motion by connecting single actuator modules in series [48]. A new soft SMA actuator was developed, capable of fast bending actuation with large deformations. Multiple thin SMA wires were used to increase heat dissipation for faster cooling, and the bending driving frequency of an SMA wire was increased up to 35 Hz [49].

SMAs have been widely used in a diverse range of humanoid-robotic applications since the 1980s, especially in artificial muscles, because SMA wire actuators can mimic human muscle. For example, many researchers created a dexterous robot manipulator that can mimic the human hand using SMAs. A recent study by Thayer and Priya [50] divided the robot hand into several categories based on locomotion styles and multi-DOF. For the design of a facial-expressive baby robot, SMAs were embedded in the skull of a humanoid head and connected to the elastomeric skin at control points. The SMA wires, with 35 routine pulleys were used as the skull actuators [51]. Recently, the majority of SMA robotic researchers have been more interested in biologically inspired (or biometric) robotics, as these robots are useful in solving problems that are challenging for humans by providing pertinent information from underwater, space, air, and land. The state-of-the-art robotic applications using SMA wire actuators are summarized in Table 3, while emphasizing biomimetic robot applications.

Over the last decades, SMAs have been utilized as alternative actuators for underwater robots due to their ability to perform flexible and complex movements, inspired by biological mechanisms [52]. Wang et al. [53,54] designed a micro-robot fish driven by a flexible actuated biomimetic fin that

simulates the musculature, and flexible bending, of a squid/cuttlefish. Rossi et al. [55] suggested a new concept, using V-shape configured SMA actuators to bend a continuous flexible structure, representing the backbone of a robot fish. A small crawling robot has been developed by mimicking the model organism of *Caenorhabditis elegans* [56]. A thermal SMA was selected as an actuator because of having properties similar to those of *C. elegans* muscles. The starfish robot has a number of tentacles or arms extending from its central body in the form of a disk, like the topology of a real starfish. The arm is a soft and composite structure, generating a planar reciprocal motion with a fast response speed upon actuation provided by the SMA wires [57,58]. An SMA composite-based soft actuator was designed to provide a large deformation profile inspired by the contraction of a jellyfish bell, utilizing the rowing mechanism for locomotion (e.g., buoyance) [59]. This actuator was found to achieve 80% of maximum deformation, consuming 7.9 J/cycle when driven at 16.2 V/0.98 A and a frequency of 0.25 Hz [59]. Marut et al. [60] designed another type of jellyfish-inspired jet propulsion robot (JetPRo) mimicking the proficient jetting propulsion mechanism (iris mechanism) used by the hydromedusa *Sarsia tubulosa*. A biomimetic swimming robot, based on the locomotion of a marine turtle and SMA wire, was developed by Kim et al. to perform the smooth, soft flapping motions of this type of turtle [61]. The motion of such a structure can be designed by specifying the angle between a filament of the scaffold structure, and a shape-memory alloy (SMA) wire. Based on the analysis of the *Chelonia mydas* turtle, using two swimming gaits (routine and vigorous swimming gaits), the flipper actuator was designed to be divided into three segments, containing a scaffold structure fabricated with a 3-D printer [62]. A soft-bodied robot was proposed using an SMA-based soft composite with inchworm-inspired locomotion, capable of both two-way linear and turning movement [63]. The centimeter-scale work-like robot, inspired by a helical kirigami-enabled parallel structure, was designed using an SMA coil spring actuator [64]. Unlike the inchworm-inspired locomotion, a quick actuation mechanism for a flytrap-inspired robot has been studied by using SMAs [65], which actuates artificial leaves made from asymmetrically laminated carbon fiber. Similar to the flytrap-inspired robot, a novel direction-changing concept for miniature jumping robots, inspired by Froghopper, has been developed by using a coil spring actuator for triggering the jumping [66]. SMAs acting as artificial biceps and triceps are used for mimicking the morphing wing mechanism of the bat [67], or dragonfly [68].

Table 3. Summary of state-of-the-art bio-inspired robotic applications using SMA actuators.

Robots	Biomimetic	References
Micro-fish	Fish fin	[53–55]
Crawling	*C. elegans*	[56]
Tentacle	Starfish	[57,58]
Buoyance	Jellyfish	[59,60]
Swimming	Turtle	[61,62]
Linear	Inchworm	[63,64]
Flytrap	Venus flytrap	[65]
Jumping	Froghopper	[66]
Flying	Bat, Dragonfly	[67,68]

Although SMA actuators provide several attractive advantages over traditional actuators, including silent and smooth operation, direct actuation, simple driving circuitry, and high-power density, it is well-known that there are some technical limitations, such as low energy efficiency, associated with the energy conversion of heat to mechanical work, slow response, and difficulties in positional control [69]. In particular, a complex thermal–electrical–mechanical model is required to correctly represent the behavior of the SMA described in Section 3.1. However, this is challenging because of its strong temperature dependence. The property changes will cause a significant backlash-like hysteresis loop in a highly nonlinear manner in open-loop control responses, which results in response delays and steady-state errors, and limit-cycle issues in the position control

of SMA actuators with a conventional feedback controller, such as a PID controller [70]. The robust position control of SMA actuators for compensating hysteresis is therefore one of the interesting research areas in the smart-material community. For example, the sliding mode control (SMC) was applied to control the arm positions of a flexible robot [71,72]. Advanced SMC schemes, such as an adaptive sliding-mode control with a PID tuning method [73], and an intelligent sliding mode control [74], are proposed to achieve robustness against the SMA hysteresis phenomenon. Lee et al. [75] experimentally demonstrated that a simple time delay control (SDC), without a precise actuator model, can be effective for actuating an SMA wire actuator. The open-loop pulse width modulation (PWM) control was also developed to reduce the SMA actuator energy consumption [76]. This control method with a metal-oxide-semiconductor field-effect transistor (MOSFET) switching circuit, can also be used for safely powering the SMA wire actuators across a wide range of speeds or input voltages, which will in turn ensure a better durability, by preventing overheating of the SMA wires [77]. Numerous new approaches for the design and control of SMA actuators have been explored. For example, Selden et al. [78] proposed a segmented SMA wire actuator, which is divided into many segments, and their thermal states are controlled individually as a group of finite-state machines. Then, instead of driving a current to the entire SMA wire and controlling the wire length based on the analog strain–temperature characteristics, this approach controls the binary state (hot or cold) of individual segments, which improves efficiency. The SMA wire itself can be the sensing element for the control of the SMA actuator. The classic example of this is to take advantage of the electrical resistance feedback, which eliminates the need for a position sensor, in this case by utilizing the SMA's electrical resistance feedback. The position control system for the SMA wire actuator with electrical-resistance feedback was proposed by Ma et al. [79], and has been recently advanced by Lynch et al. [80]. We use the embedded SMA wire in composites, both as an actuator and as a strain sensor. Nagai et al. [81] proposed using the SMA wire as a strain sensor to obtain an actuation trigger signal, based on the variation of the SMA electric resistance correlated with the strain.

4. Medical and Rehabilitation Applications

In recent years, robots are being actively studied for utilization in biomedical fields. Especially, various efforts have been made to apply smart fluid to the rehabilitation robot based on the characteristic that the torque can be controlled continuously with a simple system. In 2007, Weinberg et al. [82,83] reported for design and test of ER brake-based active knee rehabilitation orthotic device. The knee brace provides variable and controllable damping that foster motor recovery in stroke patients. An electrorheological fluid-based brake component is used to facilitate knee flexion during stance by providing resistance to knee buckling. The schematic diagrams of the proposed orthotic device and ER fluid-based brake are shown in Figure 8. In the early 2000s, Kim and Oh [84] developed an above knee prosthesis using a rotary MR damper and its effectiveness was evaluated by using leg simulator. It was reported that by controlling the damping force of MR damper, the desired knee joint angle can be accurately achieved. Park et al. [85] designed and manufactured a prosthetic leg for above-knee amputees using MR damper and control performance was evaluated experimentally. The proposed device includes the wearable connector, encoder, flat motor, planetary gear head, gyro sensor, hinge, and MR damper. The MR damper generates reaction force, while the electronically commutated motor actively controls the knee joint angle during gait cycle. The configuration of the proposed above knee prosthesis and photograph of the fabricated above knee prosthesis are presented in Figure 9. Furusho et al. [86] proposed an ankle–foot orthosis using controllable MR brake in 2007. They fabricated two different prototypes by applying shear mode MR brakes with maximum torque of 0.71 Nm and 11.8 Nm, respectively. It is observed that the subject could maintain the dorsal flexion and prevent the drop foot in swing phase that by controlling the ankle torque using MR brake. Additionally, it is demonstrated that the higher bending moment and shorter walking cycle could be achieved by activating MR brake that in turn can prevent drop foot in swing phase and slap foot at heel strike. Kikuchi et al. [87] improved the model developed by Fursusho et al. by adopting a

newly proposed compact size MR brake with enhanced maximum torque of 10 Nm. Avraam et al. [88] proposed portable smart wrist rehabilitation device with rotational MR fluid brake actuator for telemedicine application as shown in Figure 10. They designed a novel T-shaped MR fluid brake that can generate output torque of 22.5 Nm and adopted to the proposed portable wrist rehabilitation system. Egawa et al. [89] recently developed and tested a wearable haptic device with pneumatic artificial muscles and MR brake for the application of upper limb rehabilitation. It is observed that this haptic device can render various force senses such as elasticity, friction, and viscosity.

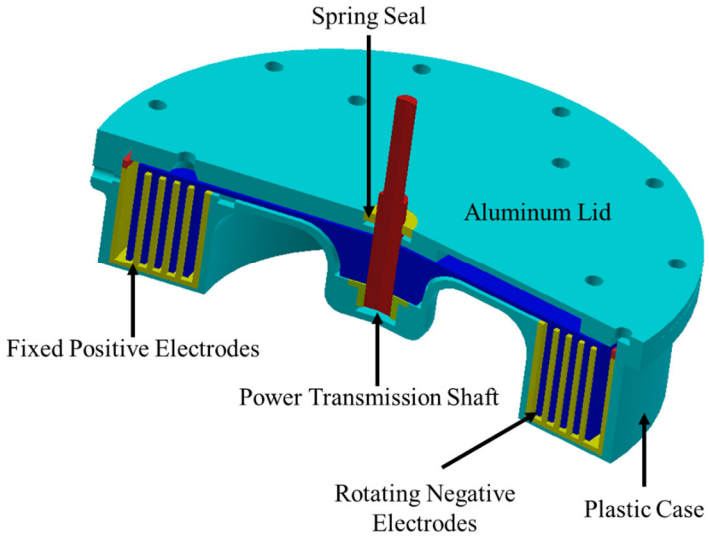

Figure 8. ER brake for active knee rehabilitation orthotic device [83].

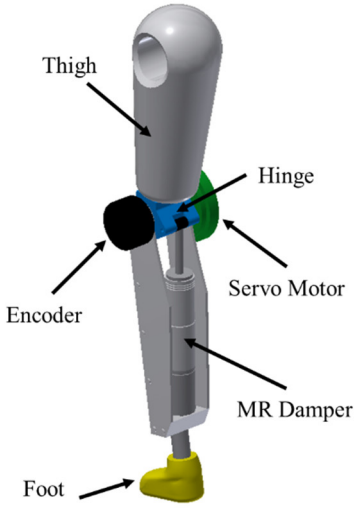

Figure 9. The configuration of above knee prosthesis using MR damper [85].

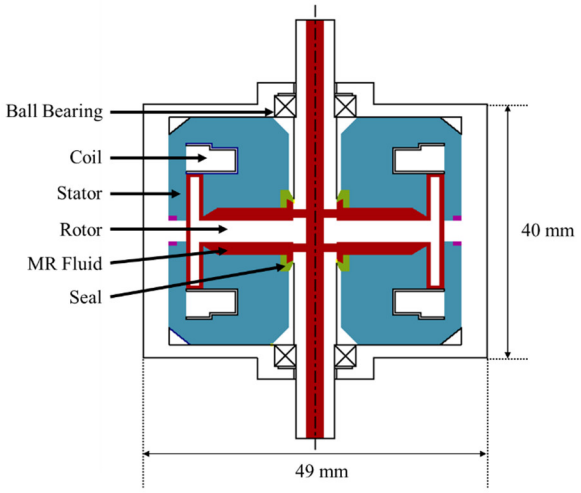

Figure 10. T-shaped MR brake for portable wrist rehabilitation device [88].

Research on the application of biomedical field using shape memory alloys is also proceeding variously. To take advantage of the shape memory effect that can generate a motion similar to human muscle behavior, many studies have been reported for SMA actuation mechanism in the prosthetic hand application. Matsubara et al. [90] reported a new prosthetic hand using SMA artificial muscles. It is demonstrated that the proposed device could grasp an object with the motion of the prosthetic finger. The photographs of the fabricated prosthetic hand and test result are presented in Figure 11. Kaplanoglu [91] proposed a tendon-driven SMA actuated finger for the prosthetic hand development that activates SMA actuation using an electro-myographic signal. In order to satisfy the requirement that a minimally-invasive surgical robot should have a large operating force in a small volume, research has been conducted to apply an SMA wire actuator to the robot end effector. Kode et al. [92] proposed a novel hybrid actuator to increase the number of degrees of freedom in minimally-invasive surgery (MIS) robots through local actuation of the end effector. The proposed system consists of a laparoscopic needle driver, SMA wire, and DC motor. The photograph of the proposed prototype is shown in Figure 12. The designed actuator is 5 mm in diameter and 40 mm in length and is used to actuate 10 mm long needle driver jaws, while generating a force of 15 N and a gripping force of 5.5 N. Giataganas et al. [93] reported prototype of minimally invasive surgery robotic tool using SMA wires in an antagonistic tendon configuration to obtain low stiffness. It is observed that the low weight (150 g) of the proposed tool could make it suitable for most surgical operations.

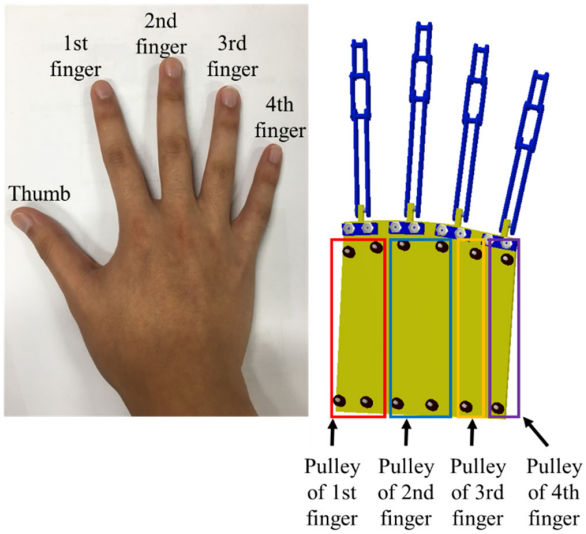

Figure 11. Prosthetic hand with SMA actuator [90].

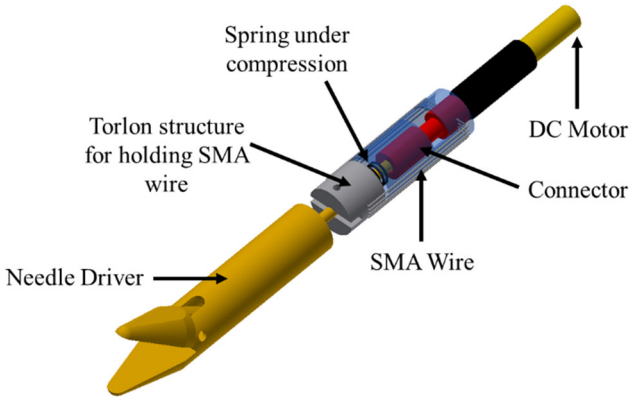

Figure 12. SMA wire-based end-effector for minimally invasive surgery [91].

5. Conclusions and Future Direction

This topical review presents state-of-the-art developments of robotic applications using smart materials. Smart materials used for robotic applications include electro-rheological (ER) fluids, magneto-rheological (MR) fluids, and shape memory alloys (SMAs). As reviewed, these smart materials can be effectively used as actuators for various types of robots, but there exist still many material and technical limitations for practical implementation. Both ERF and MRF are very effective to devise special robots such as leg robot in which unwanted vibrations need to be controlled in real time. To successfully realize those special robots in practical environment, the higher level of the field-dependent yield stress, the higher robustness to impurities, the wider temperature range, the less abrasiveness and wear properties, and the prevention of particle sedimentation are essentially required to be resolved or improved. Bio-inspired small-scale soft robotics using SMAs are very promising candidates for practical use because of their artificial muscle properties with large strain variation. However, in order to apply SMAs to robots, the narrow bandwidth issue associated with the asymmetric actuation property should be first resolved. Moreover, continuous improvement on their controllability, stability, and large actuation force are still essential to be ensured for future-oriented robot applications associated with SMA actuator. This review article has covered recent advances and trends on robotic applications using diverse smart materials.

The words representing future robots will be 'artificial intelligence' and 'natural mimicking', and the implementation of natural mimicking is proceeding in the form of soft robotics. Soft robotics is a newly emerging field of robot research. It is expected that friendly human–robot interaction will be obtained based on inherent soft characteristics. The soft robots can be adopted to their surroundings actively and can mimic the function of biological systems such as octopus leg and human muscles. The final goal of soft robotics is the integration of soft actuators, sensors, controls and power source without any rigid part. Soft materials, actuating mechanisms using the materials, and fabrication methods such as 3D printing have been extensively studied. However, there are still many challenges in the field of soft robotics. From the material aspect of the sensor and the actuator, soft and smart materials, such as shape memory alloys, shape memory polymers, electro-rheological fluids, electro-rheological elastomers, magneto-rheological fluids, magneto-rheological elastomers, and electro-active polymers (EAPs) are very important part for the successful development of soft robots. Smart materials will change the definition of a robot and the relationship between robot and human.

However, it should be noted here that the development of a new class of smart materials, which can be optimally and adaptively applicable to various robots, is still an on-going research issue. Continuous advances in the synthesis of smart materials are likely to motivate the creativity of researchers seeking to harness these materials for robotic applications. Finally, this review article provides very useful information on the potential research opportunities and emerging technologies using smart materials for the innovative robots of the future.

Author Contributions: S.-B.C. as a corresponding author takes the primary responsibility for this article. J.-W.S. and G.-W.K. drafted the manuscript, and all co-authors reviewed.

Funding: This research was funded by INHA IST-NASA Deep Space Exploration Joint Research Center (NRF-2017K1A4A3013662).

Conflicts of Interest: The authors declare no conflicts of interest.

References

1. Gandhi, M.V.; Thompson, B.S.; Choi, S.B.; Shakir, S. Electro-rheological-fluid-based articulating robotic systems Transactions of the ASME-Mechanisms. *Transm. Autom. Des.* **1989**, *111*, 328–336. [CrossRef]
2. Choi, S.B. Control of Single-Link Flexible Manipulators Fabricated from Advanced Composite Laminates and Smart Materials Incorporating Electro-Rheological Fluids. Ph.D. Thesis, Department of Mechanical Engineering, Michigan State University, East Lansing, MI, USA, 1990.
3. Choi, S.B.; Thompson, B.S.; Gandhi, M.V. Experimental control of a single-link flexible arm incorporating electrorheological fluids. *J. Guid. Control Dyn.* **1995**, *18*, 916–919. [CrossRef]
4. Choi, S.B.; Han, S.; Kim, H.K.; Cheong, C.C. H-infinity control of a flexible gantry robot arm using smart actuators. *Mechatronics* **1999**, *9*, 271–286. [CrossRef]
5. Han, S.S.; Choi, S.B.; Kim, J.H. Position control of a flexible gantry robot arm using smart material actuators. *J. Robot. Syst.* **1999**, *16*, 581–595. [CrossRef]
6. Monkman, G.J. An electrorheological tactile display. *Presence Mass. Inst. Technol.* **1992**, *1*, 219–228. [CrossRef]
7. Shafer, A.S.; Kermani, M.R. On the feasibility and suitability of MR and ER based actuators in human friendly manipulators. In Proceedings of the 2009 IEEE/RSJ Ternational Conference on Intelligent Robots and Systems, St. Louis, IL, USA, 11–15 October 2009.
8. LORD Company. Available online: http://www.lord.com/ (accessed on 1 July 2018).
9. Choi, S.B.; Han, Y.M. *Magnetorheological Fluid Technology: Applications in Vehicle Systems Taylor & Francis Group*; CRC Press: Boca Raton, FL, USA, 2012.
10. Kordonsky, W.I.; Gorodkin, S.R.; Kolomentsev, A.V.; Kuzmin, V.A.; Luk'ianovich, A.V.; Protasevich, N.A.; Prokhorov, I.V.; Shulman, Z.P.; Byelocorp Scientific Inc. Magnetorheological Valve and Devices Incorporating Magnetorheological Elements. U.S. Patent No. 5353839, 11 October 1994.
11. Yadmellat, P.; Kermani, M.R. Adaptive Control of a Hysteretic Magneto-rheological robot actuator. *IEEE/ASME Trans. Mechatron.* **2016**, *21*, 1336–1344. [CrossRef]
12. Jolly, M.R.; Bryan, S.R. Magnetorheological Grip for Handheld Implements. U.S. Patent No. 6158910, 12 December 2000.
13. Pattersson, A.; Davis, S.; Gray, J.O.; Dodd, T.J.; Ohlsson, T. Design of a magnetorheological robot gripper for handling of delicate food products with varying shapes. *J. Food Eng.* **2010**, *98*, 332–338. [CrossRef]
14. Nguyen, Q.H.; Choi, S.B.; Lee, Y.S.; Han, M.S. Optimal design of a new 3D haptic gripper for telemanipulation, featuring magnetorheological fluid brakes. *Smart Mater. Struct.* **2013**, *22*, 015009. [CrossRef]
15. Scilingo, E.P.; Sgambelluri, N.; Rossi, D.; Bicchi, A. A Towards a haptic black box for free-hand softness and shape exploration. In Proceedings of the 2003 IEEE International Conference on Robotics and Automation, Taipei, Taiwan, 14–19 September 2003.
16. Blake, J.; Gurocak, H.B. Haptic glove with MT brakes for virtual reality. *IEEE/ASME Tans. Mechatron.* **2009**, *14*, 606–615. [CrossRef]
17. Ahmadkhanlou, F.; Washington, G.N.; Bechtel, S.E. The development of a five DOF magnetorheological fluid-based telerobotic haptic system. In Proceedings of the Modeling, Signal Processing, and Control for Smart Structures, San Diego, CA, USA, 9–12 March 2008; Volume 692604. [CrossRef]
18. Walker, D.S.; Thoma, D.J.; Niemeyer, G. Variable impedence magnetorheological clutch actuator and telerobotic implementation. In Proceedings of the 2009 IEEE/RSJ International Conference on Intelligent Robots and Systems, St. Louis, IL, USA, 11–15 October 2009; pp. 2885–2891.
19. Diaz, I.; Gill, J.J.; Sanchez, E. Lower-limb robotic rehabilitation:literature review and challenges. *J. Robot.* **2011**, *2011*, 759764. [CrossRef]
20. Kikuchi, T.; Oda, K.; Yamaguchi, S.; Furusho, J. Leg-robot with MR clutch to realize virtual spastic movements. *J. Intell. Mater. Syst. Struct.* **2010**, *21*, 1523–1529. [CrossRef]

21. Kikuchi, T.; Oda, K.; Furusho, J. Leg-robot for demonstration of spastic movements of brain-injured patients with compact megnetorheological fluid clutch. *Adv. Robot.* **2010**, *24*, 671–686. [CrossRef]
22. Jiang, N.; Sun, S.; Ouyang, Y.; Xu, M.; Li, W.; Zhang, S. A highly adaptive magnetorheological fluid robotic leg for efficient terrestrial locomotion. *Smart Mater. Struct.* **2016**, *25*, 095019. [CrossRef]
23. Saito, T.; Ikeda, H. Development of normally closed type of magnetorheological clutch and its application to safe torque control system of human-collaborative robot. *J. Intell. Mater. Syst. Struct.* **2007**, *18*, 1181–1185. [CrossRef]
24. Ahmed, R.M.; Kalaykov, I.G.; Ananiev, A.V. Modeling of magneto rheological fluid actuator enabling safe human-robot interaction. In Proceedings of the IEEE International Conference on Emerging Technologies and Factory Automation, Hamburg, Germany, 15–18 September 2008. [CrossRef]
25. Ahmed, M.R.; Kalaykov, I. Semi-active compliant robot enabling collision safety for human robot interaction. In Proceedings of the 2010 IEEE International Conference on Mechatronics and Automation, Xi'an, China, 4–7 August 2010.
26. Fauteux, P.; Lauria, M.; Heintz, B.; Michaud, F. Dual-differential rheological actuator for high-performance physical robotic interaction. *IEEE Trans. Robot.* **2010**, *26*, 607–618. [CrossRef]
27. Shafer, A.; Kermani, M.R. Design and validation of a magneto-rheological clutch for practical control application in human-friendly manipulation. In Proceedings of the 2011 IEEE International Conference on Robotics and Automation, Shanghai, China, 9–13 May 2011.
28. Shafer, A.; Kermani, M.R. On the feasibility and suitability of MR fluid clutches in human-friendly manipulators. *IEEE/ASME Trans. Mechatron.* **2011**, *16*, 1073–1082. [CrossRef]
29. Hoyle, A.; Arzanpour, S.; Shen, Y. A novel magnetorheological damper based parallel planar manipulator design. *Smart Mater. Struct.* **2010**, *19*, 055028. [CrossRef]
30. Wiltsie, N. A Controllably Adhesive Climbing Robot Using Magnetorheological Fluid. Masters' Thesis, Department of Mechanical Engineering, Massachusetts Institute of Technology, Cambridge, MA, USA, September 2012.
31. Yue, M.; Liu, B.Y. Design of adaptive sliding mode control for spherical robot based on MR fluid actuator. *J. Vibroeng.* **2012**, *14*, 196–204.
32. Schmitz, G.W. Hydraulically Energized Magnetorheological Replicant Muscle Tissue and System and a Method for Using and Controlling Same. U.S. Patent No. 6168634, 2 January 2001.
33. Kashima, S.; Miyasaka, F.; Hirata, K. Novel soft actuator using magnetorheological elastomer. *IEEE Trans. Magn.* **2012**, *48*, 1649–1652. [CrossRef]
34. Zimmermann, K.; Bohm, V.; Zeidis, I. Vibration-driven mobile robot based on magneto-sensitive elastomers. In Proceedings of the 2011 IEEE/ASME International Conference on Advanced Intelligent Mechatronics, Budapest, Hungary, 3–7 July 2011.
35. Flexible Solutions. Available online: http://www.dynalloy.com (accessed on 10 July 2018).
36. Sun, L.; Huang, W.M.; Ding, Z.; Zhao, Y.; Wang, C.C.; Purnawali, H.; Tang, C. Stimulus-responsive shape memory materials: A review. *Mater. Des.* **2012**, *33*, 577–640. [CrossRef]
37. Jani, J.M.; Leary, M.; Subic, A.; Gibson, M.A. A review of shape memory alloy research, applications and opportunities. *Mater. Des.* **2014**, *56*, 1078–1113. [CrossRef]
38. Follador, M.; Cianchetti, M.; Arienti, A.; Laschi, C. A general method for the design and fabrication of shape memory alloy active spring actuators. *Smart Mater. Struct.* **2012**, *21*, 115029. [CrossRef]
39. An, S.; Ryu, J.; Cho, M.; Cho, K. Engineering design framework for a shape memory alloy coil spring actuator using a static two-state model. *Smart Mater. Struct.* **2012**, *21*, 055009. [CrossRef]
40. Flemming, L.; Mascaro, S. Analysis of hybrid electric/thermofluidic inputs for wet shape memory alloy actuators. *Smart Mater. Struct.* **2013**, *22*, 014015. [CrossRef]
41. Zhang, X.; Hu, J.; Mao, S.; Dong, E.; Yang, J. Design and property analysis of a hybrid linear actuator based on shape memory alloy. *Smart Mater. Struct.* **2014**, *23*, 125004. [CrossRef]
42. Leng, J.; Yan, X.; Zhang, X.; Huang, D.; Gao, Z. Design of a novel flexible shape memory alloy actuator with multilayer tubular structure for easy integration into a confined space. *Smart Mater. Struct.* **2016**, *25*, 025007. [CrossRef]
43. Shim, J.; Quan, Y.; Wang, W.; Rodrigue, H.; Song, S.; Ahn, S.H. A smart soft actuator using a single shape memory alloy for twisting actuation. *Smart Mater. Struct.* **2015**, *24*, 125033. [CrossRef]

44. Sheng, J.; Desai, J.P. Design, modeling and characterization of a novel meso-scale SMA-actuated torsion actuator. *Smart Mater. Struct.* **2015**, *24*, 105005. [CrossRef]
45. Rodrigue, H.; Wei, W.; Bhandari, B.; Ahn, S.H. Fabrication of wrist-like SMA-based actuator by double smart soft composite casting. *Smart Mater. Struct.* **2015**, *24*, 125003. [CrossRef]
46. Paik, J.K.; Hawkes, E.; Wood, R.J. A novel low-profile shape memory alloy torsional actuator. *Smart Mater. Struct.* **2010**, *19*, 125014. [CrossRef]
47. Paik, J.K.; Wood, R.J. A bidirectional shape memory alloy folding actuator. *Smart Mater. Struct.* **2012**, *21*, 065013. [CrossRef]
48. Shin, B.H.; Jang, T.; Ryu, B.J.; Kim, Y. A modular torsional actuator using shape memory alloy wires. *J. Intell. Mater. Syst. Struct.* **2016**, *12*, 1658–1665. [CrossRef]
49. Song, S.; Lee, J.; Rodrigue, H.; Choi, I.; Kang, Y.J.; Ahn, S.H. 35 Hz shape memory alloy actuator with bending-twisting mode. *Sci. Rep.* **2016**, *6*, 21118. [CrossRef] [PubMed]
50. Thayer, N.; Priya, S. Design and implementation of a dexterous anthropomorphic robotic typing (DART) hand. *Smart Mater. Struct.* **2011**, *20*, 035010. [CrossRef]
51. Tadesse, Y.; Hong, D.; Priya, S. Twelve Degree of Freedom Baby Humanoid Head Using Shape Memory Alloy Actuators. *J. Mech. Robot.* **2011**, *3*, 011008. [CrossRef]
52. Chu, W.; Lee, K.; Song, S.; Han, M.; Lee, J.; Kim, H.; Kim, M.; Park, Y.; Cho, K.; Ahn, S.H. Review of Biomimetic Underwater Robots Using Smart Actuators. *Int. J. Precis. Eng. Manuf.* **2012**, *13*, 1281–1292. [CrossRef]
53. Wang, Z.; Hang, G.; Li, J.; Wang, Y.; Xiao, K. A micro-robot fish with embedded SMA wire actuated flexible biomimetic fin. *Sens. Actuators A* **2008**, *144*, 354–360. [CrossRef]
54. Wang, Z.; Hang, G.; Wang, Y.; Li, J.; Du, W. Embedded SMA wire actuated biomimetic fin: A module for biomimetic underwater propulsion. *Smart Mater. Struct.* **2008**, *17*, 025039. [CrossRef]
55. Rossi, C.; Colorado, J.; Coral, W.; Barrientos, A. Bending continuous structures with SMAs: A novel robotic fish design. *Bioinspir. Biomim.* **2011**, *6*, 045005. [CrossRef] [PubMed]
56. Yuk, H.; Kim, D.; Lee, H.; Jo, S.; Shin, J.H. Ketner Shape memory alloy-based small crawling robots inspired by *C. elegans*. *Bioinspir. Biomim.* **2011**, *6*, 046002. [CrossRef] [PubMed]
57. Jin, H.; Dong, E.; Xu, M.; Liu, C.; Alici, G.; Jie, Y. Soft and smart modular structures actuated by shape memory alloy (SMA) wires as tentacles of soft robots. *Smart Mater. Struct.* **2016**, *25*, 085026. [CrossRef]
58. Jin, H.; Dong, E.; Alici, G.; Mao, S.; Min, X.; Liu, C.; Low, K.H.; Yang, J. A starfish robot based on soft and smart modular structure (SMS) actuated by SMA wires. *Bioinspir. Biomim.* **2016**, *11*, 056012. [CrossRef] [PubMed]
59. Villanueva, A.; Smith, C.; Priya, S.A. A biomimetic robotic jellyfish (Robojelly) actuated by shape memory alloy composite actuators. *Bioinspir. Biomim.* **2011**, *6*, 036004. [CrossRef] [PubMed]
60. Marut, K.; Stewart, C.; Michael, T.; Villanueva, A.; Priya, S. A jellyfish-inspired jet propulsion robot actuated by an iris mechanism. *Smart Mater. Struct.* **2013**, *22*, 094021. [CrossRef]
61. Kim, H.; Song, S.; Ahn, S.H. A turtle-like swimming robot using a smart soft composite (SSC) structure. *Smart Mater. Struct.* **2013**, *22*, 014007. [CrossRef]
62. Song, S.; Kim, M.; Rodrigue, H.; Lee, J.; Shim, J.; Kim, M.; Chu, W.; Ahn, S.H. Turtle mimetic soft robot with two swimming gaits. *Bioinspir. Biomim.* **2016**, *11*, 036010. [CrossRef] [PubMed]
63. Wang, W.; Lee, J.; Rodrigue, H.; Song, S.; Chu, W.; Ahn, S.H. Locomotion of inchworm-inspired robot made of smart soft composite (SSC). *Bioinspir. Biomim.* **2014**, *9*, 046006. [CrossRef] [PubMed]
64. Zhang, K.; Qiu, C.; Dai, J.S. Helical kirigami-enabled centimeter-scale worm robot with shape-memory-alloy linear actuators. *J. Mech. Robot.* **2015**, *7*, 021014. [CrossRef]
65. Kim, S.; Koh, J.; Lee, J.; Ryu, J.; Cho, M.; Cho, K. Flytrap-inspired robot using structurally integrated actuation based on bistability and a developable surface. *Bioinspir. Biomim.* **2014**, *9*, 036004. [CrossRef] [PubMed]
66. Jung, G.; Cho, K. Froghopper-inspired direction-changing concept for miniature jumping robots. *Bioinspir. Biomim.* **2016**, *11*, 056015. [CrossRef] [PubMed]
67. Colorado, J.; Barrientos, A.; Rossi, C.; Bahlman, J.W.; Breuer, K.S. Biomechanics of smart wings in a bat robot: Morphing wings using SMA actuators. *Bioinspir. Biomim.* **2013**, *7*, 036006. [CrossRef] [PubMed]
68. Festo. *BionicOpter—Inspired by Dragonfly Flight*; Festo: Esslingen am Neckar, Germany, 2013.
69. Dimitris, C.L. *Shape Memory Alloys: Modeling and Engineering Applications*; Springer: Berlin, Germany, 2008.

70. Mohammad, H.E.; Hashem, A. Nonlinear control of a shape memory alloy actuated manipulator. *J. Vib. Acoust.* **2002**, *124*, 566–575.
71. Price, A.D.; Jenifene, A.; Naguib, H.E. Design and control of a shape memory alloy based dexterous robot hand. *Smart Mater. Struct.* **2007**, *16*, 1401. [CrossRef]
72. Choi, S.B. Position control of a single-link mechanism activated by shape memory alloy springs: Experimental results. *Smart Mater. Struct.* **2006**, *15*, 51. [CrossRef]
73. Taril, N.T.; Ahn, K.K. Adaptive proportional–integral–derivative tuning sliding mode control for a shape memory alloy actuator. *Smart Mater. Struct.* **2011**, *20*, 055010.
74. Hannen, J.C.; Crews, J.H.; Buckner, G.D. Indirect intelligent sliding mode control of a shape memory alloy actuated flexible beam using hysteretic recurrent neural networks. *Smart Mater. Struct.* **2012**, *21*, 085015. [CrossRef] [PubMed]
75. Lee, H.J.; Lee, J.J. Time delay control of a shape memory alloy actuator. *Smart Mater. Struct.* **2004**, *13*, 227. [CrossRef]
76. Ma, N.; Song, G. Control of shape memory alloy actuator using pulse width modulation. *Smart Mater. Struct.* **2003**, *12*, 712. [CrossRef]
77. A Revolution In Motion! Available online: http://migamotors.com/ (accessed on 20 July 2018).
78. Selden, B.; Cho, K.; Asada, H.H. Segmented shape memory alloy actuators using hysteresis loop control. *Smart Mater. Struct.* **2006**, *15*, 642. [CrossRef]
79. Ma, N.; Song, G.; Lee, H.-J. Position control of shape memory alloy actuators with internal electrical resistance feedback using neural networks. *Smart Mater. Struct.* **2004**, *13*, 777. [CrossRef]
80. Lynch, B.; Jiang, X.X.; Ellery, A.; Nitzsche, F. Characterization, modeling, and control of Ni-Ti shape memory alloy based on electrical resistance feedback. *J. Intell. Mater. Syst. Struct.* **2016**, *27*, 2489–2507. [CrossRef]
81. Nagai, H.; Oishi, R. Shape memory alloys as strain sensors in composites. *Smart Mater. Struct.* **2006**, *15*, 493. [CrossRef]
82. Weinberg, B.; Nikitczuk, J.; Patel, S.; Patritti, B.; Mavroidis, C.; Bonato, P.; Canavan, P. Design, Control and Human Testing of an Active Knee Rehabilitation Orthotic Device. In Proceedings of the 2007 IEEE International Conference on Robotics and Automation, Roma, Italy, 10–14 April 2007; pp. 4126–4133.
83. Nikitczuk, J.; Weinberg, B.; Canavan, P.K.; Mavroidis, C. Active knee rehabilitation orthotic device with variable damping characteristics implemented via an electrorheological fluid. *IEEE/ASME Trans. Mechatron.* **2010**, *15*, 952–960. [CrossRef]
84. Kim, J.H.; Oh, J.H. Development of an above knee prosthesis using MR damper and leg simulator. In Proceedings of the IEEE International Conference on Robotics and Automation (ICRA), Seoul, Korea, 21–26 May 2001; pp. 43686–43691.
85. Park, J.; Yoon, G.H.; Kang, J.W.; Choi, S.B. Design and control of a prosthetic leg for above-knee amputees operated in semi-active and active modes. *Smart Mater. Struct.* **2016**, *25*, 085009. [CrossRef]
86. Furusho, J.; Kikuchi, T.; Tokuda, M.; Kakehashi, T.; Ikeda, K.; Morimoto, S.; Hashimoto, Y.; Tomiyama, H.; Nakagawa, A.; Akazawa, Y. Development of shear type compact MR brake for the intelligent ankle-foot orthosis and its control; research and development in NEDO for practical application of human support robot. In Proceedings of the IEEE 10th International Conference on Rehabilitation Robotics (ICORR), Noordwijk, The Netherlands, 12–15 June 2007; pp. 89–94.
87. Kikuchi, T.; Tanida, S.; Otsuki, K.; Yasuda, T.; Furusho, J. Development of third-generation intelligently controllable ankle-foot orthosis with compact MR fluid brake. In Proceedings of the IEEE International Conference on Robotics and Automation (ICRA), Anchorage, Alaska, 3–8 May 2010; pp. 2209–2214.
88. Avraam, M.; Horodinca, P.; Leiter, P.; Preumont, A. Portable Smart Wrist Rehabilitation Device driven by rotational MR-fluid brake actuator for telemedicine application. In Proceedings of the International Conference on Intelligent Robots and Systems, Nice, France, 22–26 September 2008; pp. 1441–1446.
89. Egawa, M.; Watanabe, T.; Nakamura, T. Development of a wearable haptic device with pneumatic artificial muscles and MR brake. In Proceedings of the IEEE Virtual Reality Conference 2015, Minneapolis, MN, USA, 29 March–2 April 2015; pp. 173–174.
90. Matsubara, S.; Okamoto, S.; Lee, J. Prosthetic hand using shape memory alloy type artificial muscle. In Proceedings of the International MultiConference of Engineers and Computer Scientists, Hong Kong, China, 14–16 March 2012; Volume 2, pp. 873–876.

91. Kaplanoglu, E. Design of shape memory alloy-based and tendon-driven actuated fingers towards a hybrid anthropomorphic prosthetic hand. *Int. J. Adv. Robot. Syst.* **2012**, *9*, 77. [CrossRef]
92. Kode, V.R.C.; Cavusoblu, M.C.; Azar, M.T. Design and characterization of a novel hybrid actuator using shape memory alloy and D.C motor for minimally invasive surgery applications. In Proceedings of the IEEE International Conference on Mechatronics and Automation 2005, Niagara Falls, ONT, Canada, 29 July–1 August 2005; pp. 416–420.
93. Giataganas, P.; Evangeliou, N.; Koveos, Y.; Kelasidi, E.; Tzes, A. Design and experimental evaluation of an innovative SMA-based tendon-driven redundant endoscopic robotic surgical tool. In Proceedings of the 19th Mediterranean Conference on Control and Automation 2011, Corfu, Greece, 20–23 June 2011; pp. 1071–1075.